CT SCANS OF A CONGLOMERATE CORE

Cameron D. Grace and Robert R. Stewart

ABSTRACT

Recently, x-ray computed tomography (CT) has been used as a petrophysical core analysis tool. This paper summerizes the basic theory behind CT as well as its use in petrophysical analysis. We have used scans of a conglomerate core and a Landmark workstation for display purposes. An outline of how the CT data was loaded and displayed using Landmark's 3Dplus seismic interpretation software is given.

INTRODUCTION

X-ray computed tomograghy (CT) is a radiological imaging technique that measures density and atomic composition inside opaque objects (Wellington, 1987). CT scanning was developed in the early 1970's by Hounsfield and Cormack for which they were awarded the 1979 Nobel Prize (Herman, 1980). Although originally designed for medical purposes, scientist's have used CT scanning to analyze rock cores. They have studied fluid flow in porous media (Hunt et al., 1988, Wang, 1984) and they have used CT as a core analysis tool (Wellington and Vinegar, 1987 and Hunt et al., 1988).

The purpose of this study is to conduct a preliminary investigation of a rock core through the use of CT data and a Landmark workstation. Tomotechnology of Calgary has scanned a core from the carrot creek area for the CREWES project. The core is a chert-quartz conglomerate containing siderite nodules.

DESCRIPTION OF CT SCANNER

The scanner used by Tomotechnology is a EMI CT5005 which is classified as a second generation scanner due to it's translation-rotation configuration as shown in Figure 1. This scanner has a fixed anode x-ray tube with tungsten source and thirty detectors composed of sodium iodide scintillation crystals coupled to photomultipliers. This second generation scanner differs from first generations by having a modified fan x-ray beam such that there is a collimated beam for each of the thirty detectors compared to only one beam and one detector for the first generation scanners. This configuration allows thirty adjacent paths through the core to be sampled at the same time. Superimposed on this is a linear translation of the tube and detectors. Each image requires the x-ray tube and detectors to translate eighteen times, ten degrees apart. The cross- sectional images are made up of a matrix of x-ray attenuation coefficients which have been determined by the scanner's computer.

For this study, the core was radially scanned every five millimetres for a total of twenty slices at two different energies. The two energies correspond to tube kilovoltages of 110 kVp and 140 kVp. The x-ray fan beam's thickness was three millimetres.
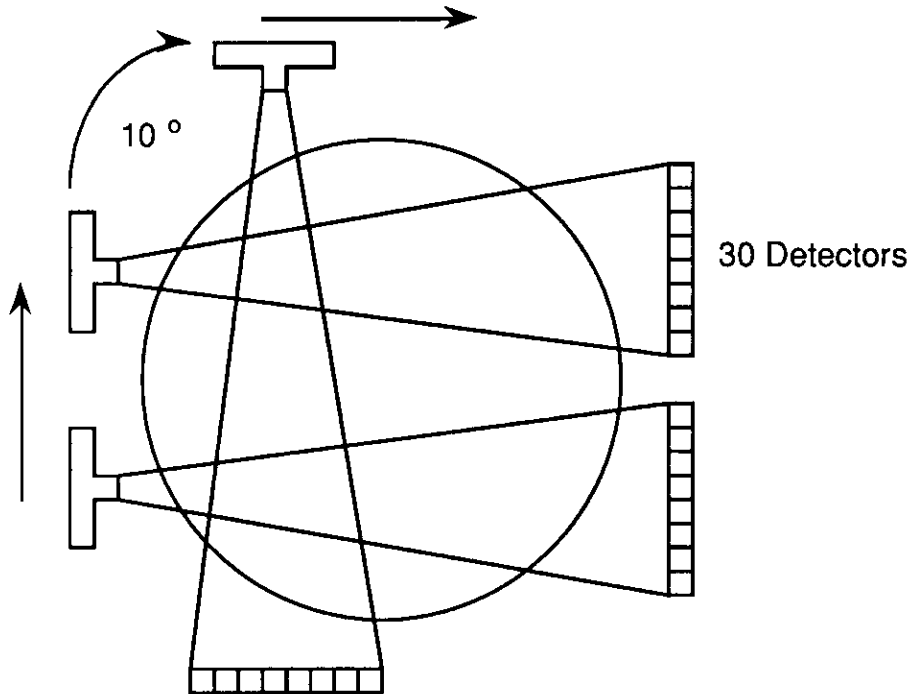
Figure 1 - CT scanner tube and detector configuration.

THEORY OF X-RAY ATTENUATION

The quantity measured in each picture element (pixel) of a CT image is the linear attenuation coefficient (μ), as described below. The x-ray attenuation coefficient is defined from Beer's law:

$$I = I_0 exp(-\mu L) \tag{1}$$

where I_0 is the incident x-ray intensity and I is the intensity after the x-ray passes through a path length L of material. The linear attenuation coefficient depends upon both electron density (bulk density), ρ, and effective atomic number, Z_e, by the equation:

$$\mu = \rho(a + bZ_e^{3.8}/E^{3.2}) \tag{2}$$

where b is a constant and a is the nearly energy-independent Klein-Nishina coefficient (Evans, 1955). The first term in equation 2 represents the Compton scattering interaction of the x-ray with the sample at energies above 100 KV. The second term of equation 2 accounts for the photoelectric absorption of x-rays, which becomes more significant at energies below 100 KV (Wellington and Vinegar, 1987).

The intensity of x-rays at the detector depends upon the sum of all the linear attenuation coefficients of each pixel through which the x-ray passes. This can be represented by:

173

$$I = I_o \exp\left\{ \sum_{i=1}^{n} \mu_i L_i \right\}$$

(3)

where n equals the number of pixels the x-ray passes through.

The above equation 2 assumes a monochromatic x-ray beam (single energy) but due to practical reasons x-ray beams used are polychromatic. Because each x-ray beam contains a spectrum of energies, a phenomena called beam hardening occurs when there is preferential absorption of the lower energy x-rays by the material being scanned. This shifts the relative energy distribution of x-rays traversing the material to higher energies than originally present in the incident beam. This causes an artifact in the resulting image called 'cupping'. Cupping is a tendency for the image of a uniform object to show increased apparent density near it's perimeter. Image improvement techniques affecting the scanner and scanner software are thoroughly discussed in the current literature (see Hunt et al., 1988).

IMAGE RECONSTRUCTION

Image reconstruction requires the determination of the linear attenuation coefficients for all the volume elements along the paths between the source and detectors. Several distinct algorithms of image reconstruction have been developed, each characterized by different computational techniques and mathematical theories. The most widely used algorithm is the filtered back-projection method using convolution (Morgan, 1983). This method involves finding a convolutional function which is used to operate on the different projections such that when these adjusted projections are back-projected and summed, the background density will be eliminated. The scanner's computer used in this study utilized this technique.

Once determined, the linear attenuation coefficient is usually expressed as a decimal number. In order to ease comparisons of linear coefficients, the CT number was defined with reference to a standard material. It's defined by:

$$CT \text{ number} \equiv \frac{\mu_{material} - \mu_{standard}}{\mu_{standard}} \times K$$

(4)

where the standard material is usually water and K is a scale factor set at either 500 (old Hounsfield scale) or 1000 (new Hounsfield scale). The new Hounsfield scale is illustrated in Figure 2. The images produced by this study use new Hounsfield units.
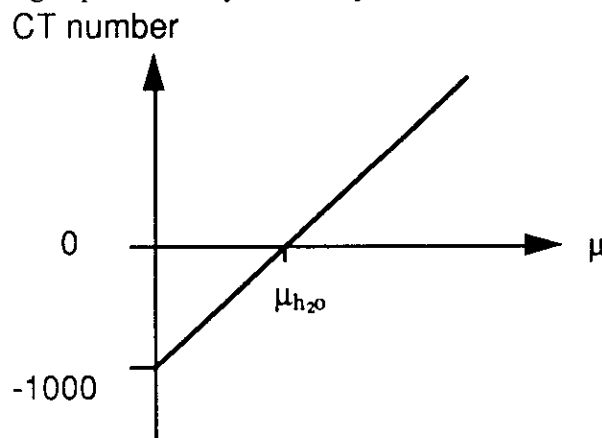
Figure 2 - New Hounsfield scale.

DISPLAY CT IMAGES

Core Description

The core (well: Texaco Amoco; location: 6-12-53-13 W5; depth: 1558.75 metres) is a chert-quartz conglomerate containing siderite nodules. The conglomerate is from the topmost lithofacies of the Pembina-Cardium Pool (Krause et al, 1987).

Data Loading

The raw CT data was transformed into SEGY format (with empty trace headers) to aid in loading into the Landmark workstation via a Perkin Elmer computer. The data was loaded into the Landmark as time series 'seismic' data. The project was set up such that 'seismic' lines represent radial slice images. This is shown in figure 3. Once the data has been loaded, a process that creates a time slice data set from the time series data is run. This enables one to display slices of the core in time. The process control files used in data loading and for time slice data set generation are in appendix A.

Image Display

Radial slices through the core are displayed as seismic lines using Landmark's seismic interpretation midpoint display. (See Figure 4 for display of ten sequential slices through the core at high energy). Longitudinal slices are reconstructed from the sequential radial slice data set along 'seismic traces' or 'time slices'. See figure 5 for a display of longitudinal slices along a trace and as a time slice. The longitudinal slice images appear stretched compared to the radial slices. This is because there are only slices every five millimetres compared to one trace (data point) every .8 millimetres. This requires a interpolation between lines (radial slices) which shows up as the smoothing or stretching in the longitudinal displays. The colour bar scale shows numbers ranging from +127 to -128. These numbers represent the CT numbers scaled down to the most significant eight bit integers.
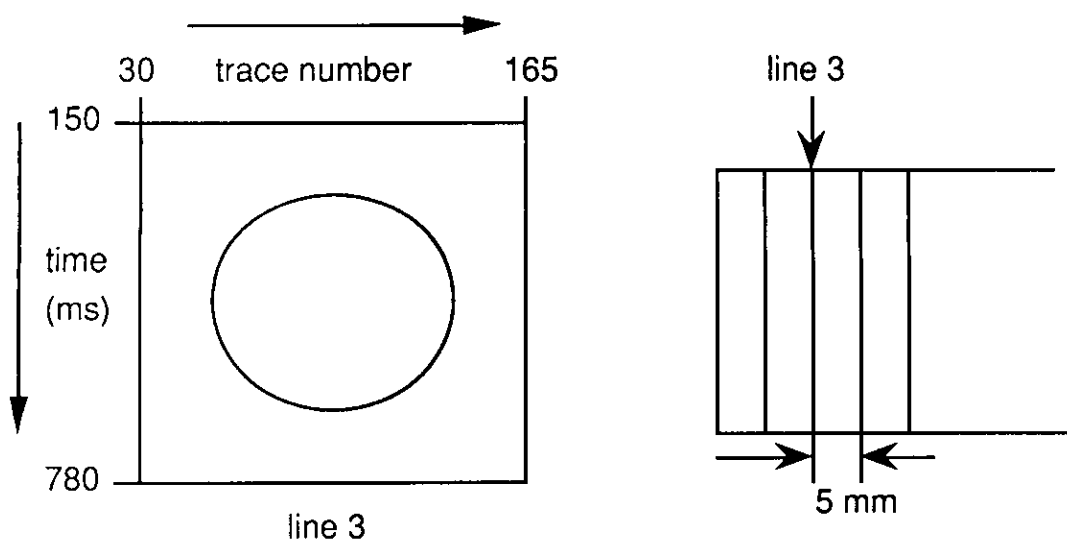
Figure 3 - Display of CT data in Landmark's format.

INTERPRETATION OF CORE

The images of the high energy CT data show the bulk density distribution of the core (See Figures 4 and 5). The higher density material has been identified as siderite which located mainly in one end of the core. The rest of the core shows a relatively uniform density distribution which is the material made up of mostly quartz and chert (See core photograph in Figure 6).

An clast of anomalous high density was found in the quartz-chert section of the core. Three slices through the clast are displayed in Figure 5. A crude attempt at image extraction of this clast was accomplished by using Landmark's fault correlation software. The clast's edges were contoured and assigned faults in a number of planes (slices) of display. Figures 7 and 8 show the clast edge contours of different slices. All of the contours were then displayed together in a 3D perspective view. This perspective display has the capability of rotating the contour data to view from different perspectives. A perspective display is shown in Figure 9.
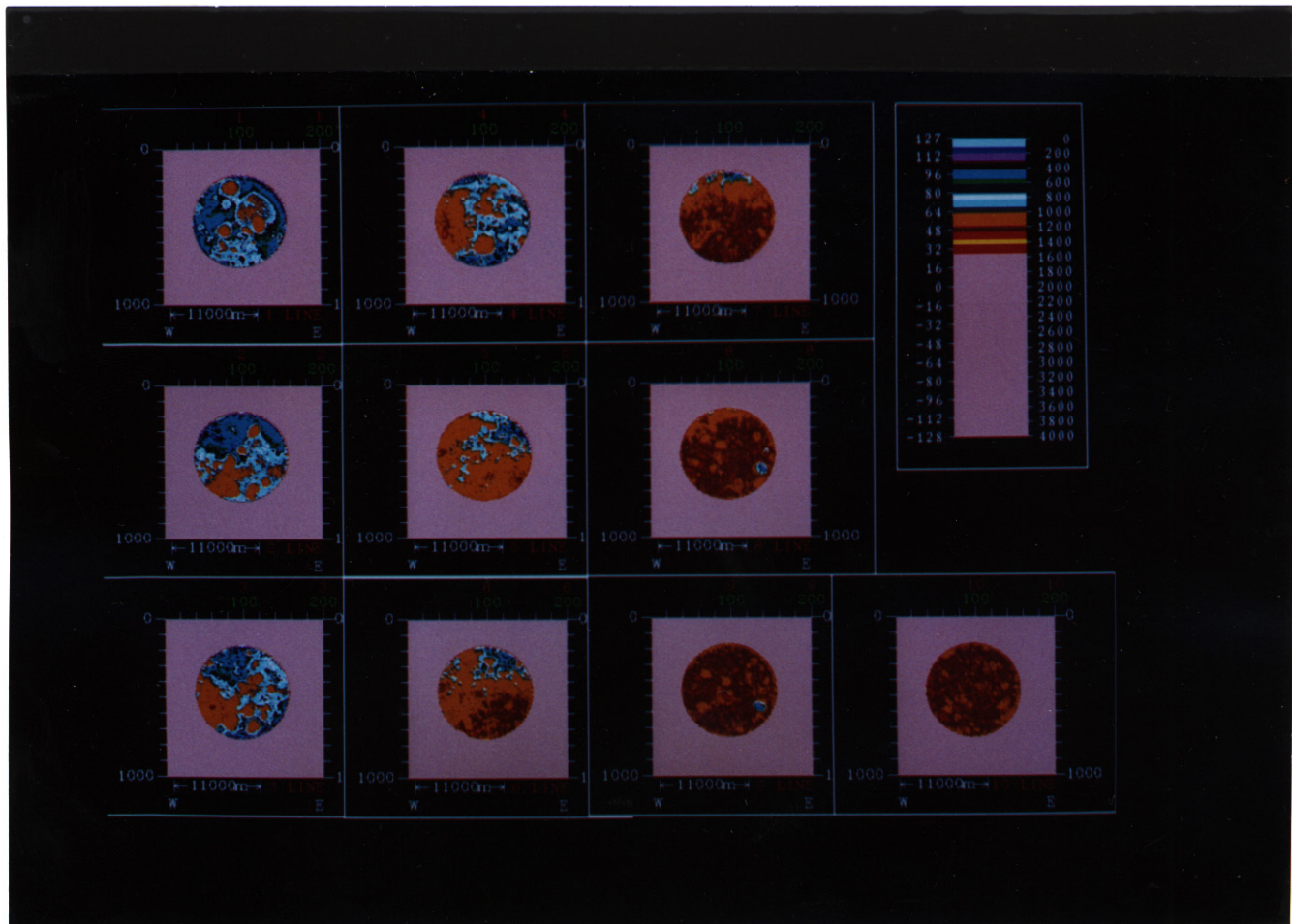

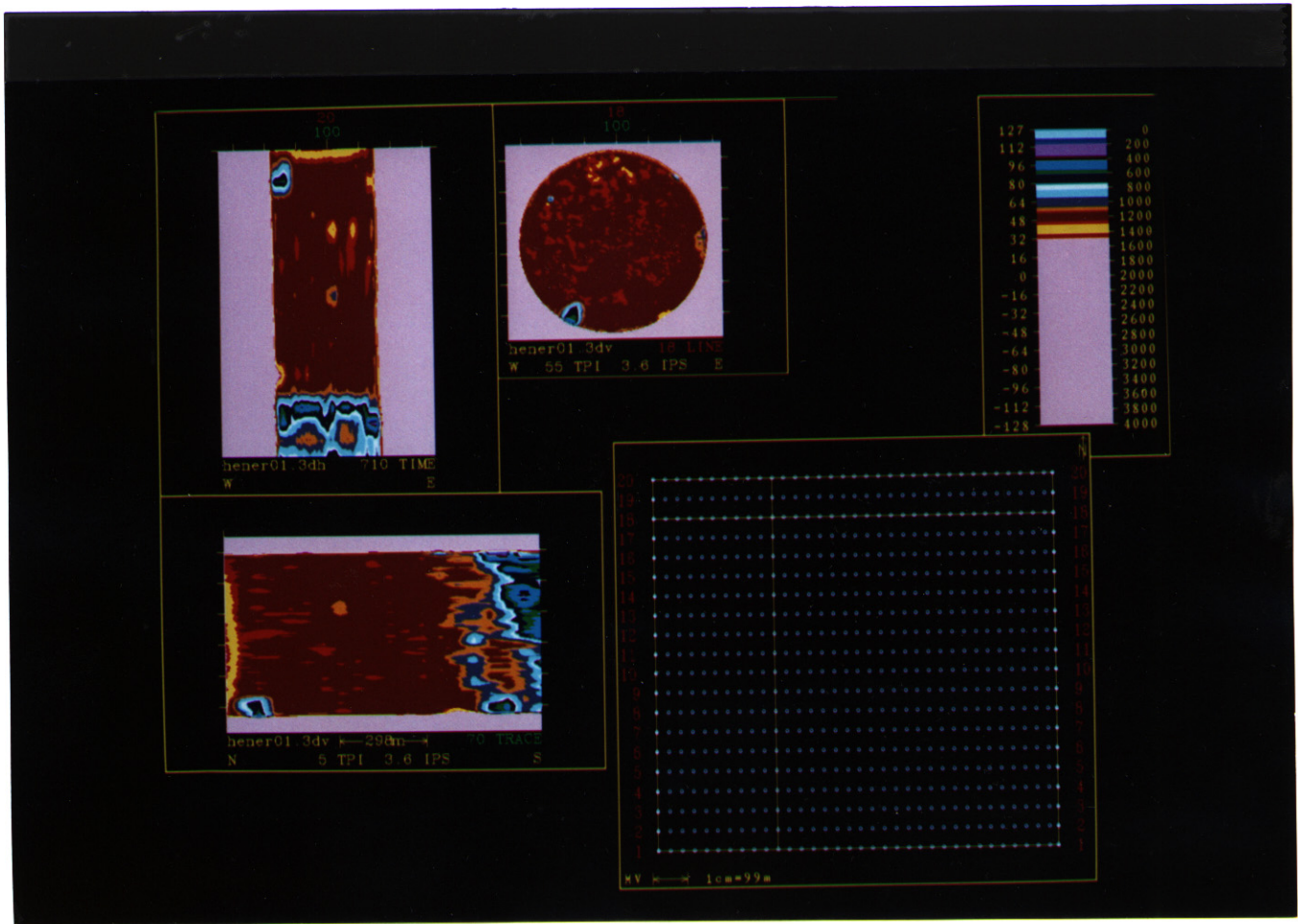Figure 4 - Ten sequential slices through core at high energy.

176

Figure 5 - Longitudinal slices of core displayed as a time slice (710 ms) and a 'seismic trace' (trace 70). Also, a radial slice through the core showing the same anomalous clast is shown (line 18).
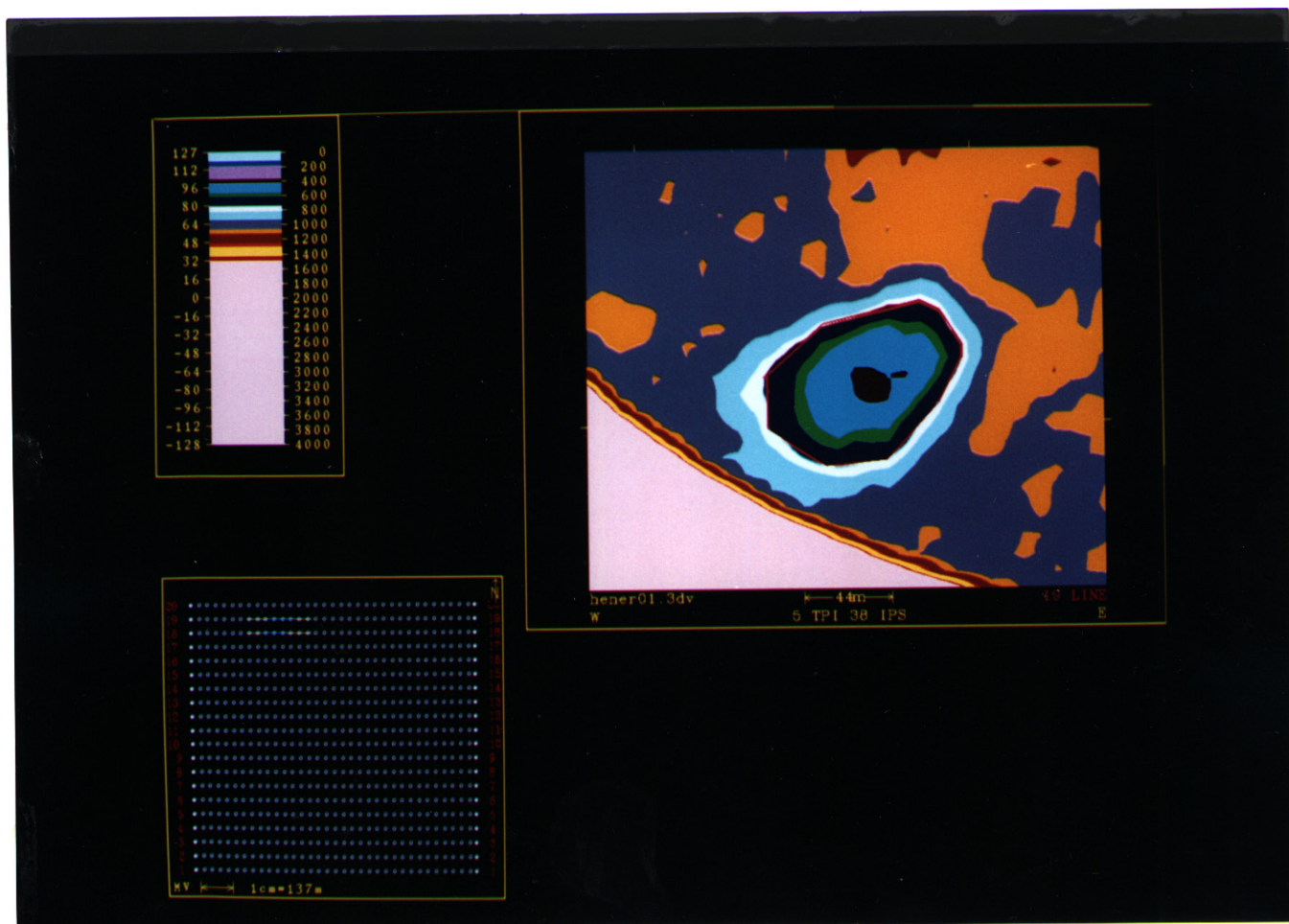
Figure 6 - Photograph of core.

Figure 7 - Partial image of a radial slice showing a clast with edge contoured using Landmark's fault correlation software package.
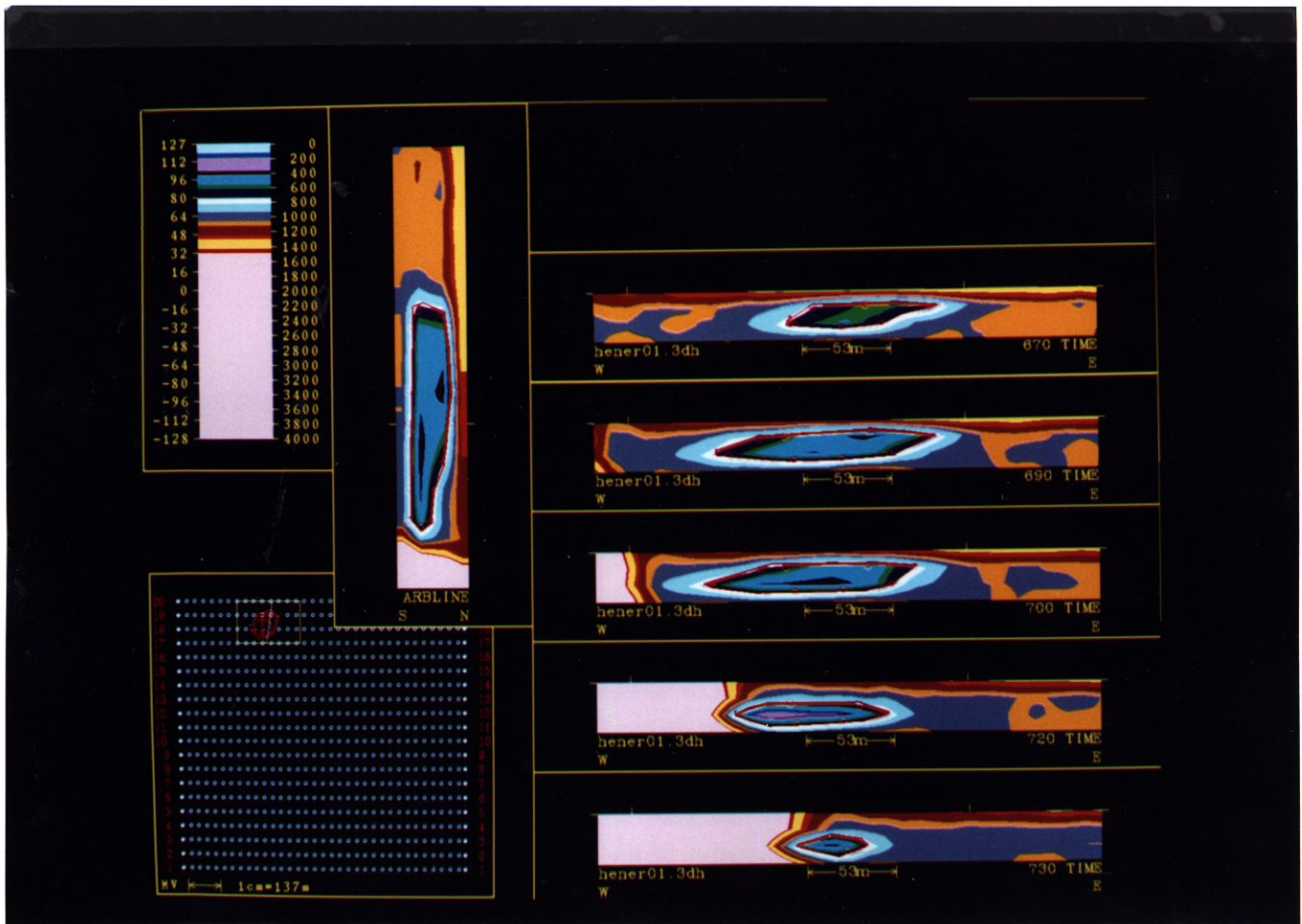
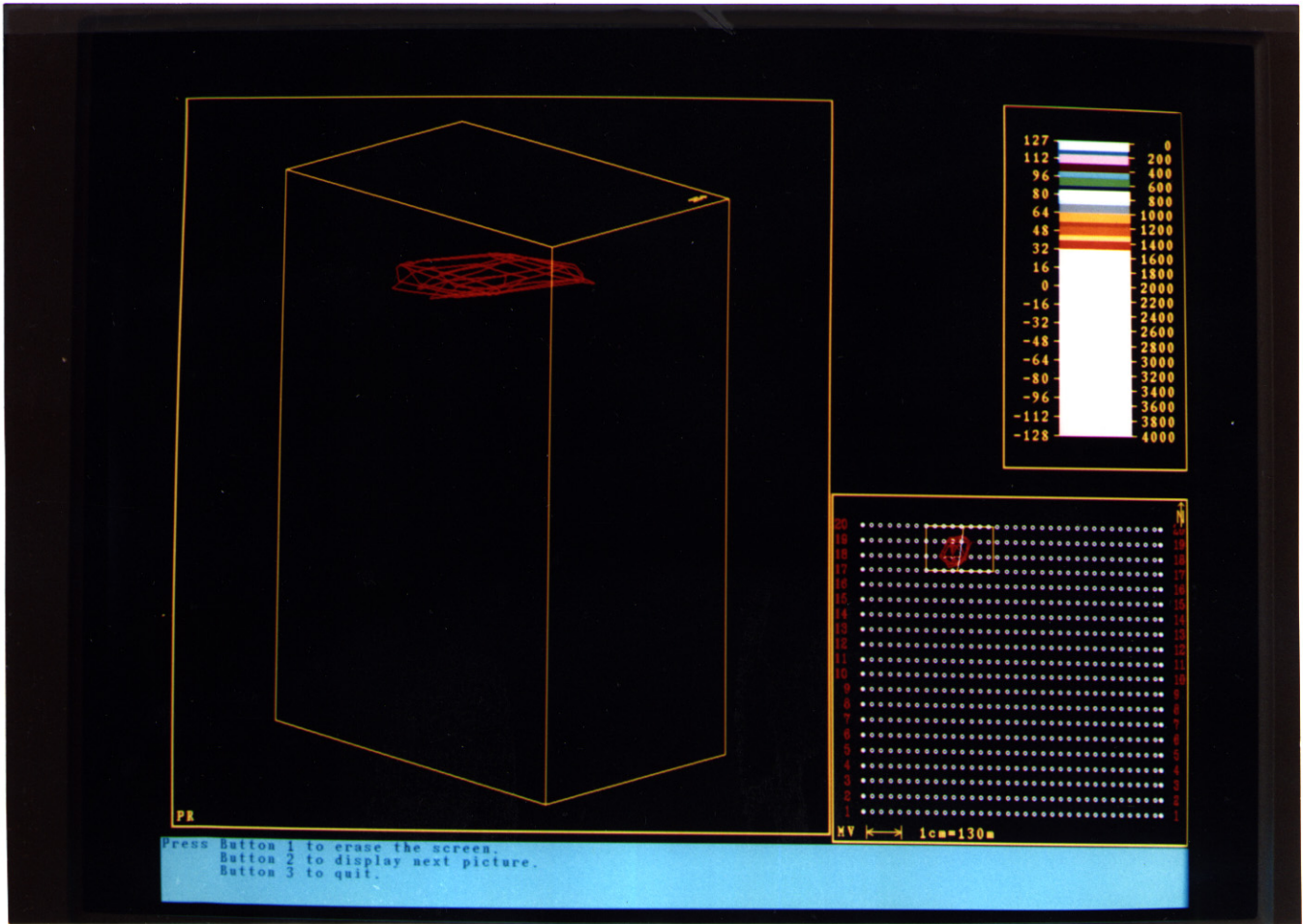Figure 8 - Partial images of time slices and an arbitrary line each showing clast edge contouring.

Figure 9 - Perspective view of contoured data.

SUMMARY

X-ray CT scanning has been used to investigate the density distribution of a conglomerate core non-destructively. The data was loaded into and displayed by a Landmark workstation using it's 3Dplus seismic interpretation software package.The data was loaded as 'seismic' time series data. Radial slices were displayed as 'seismic lines' and longitudinal slices were displayed either as 'seismic traces' or as time slices.

The CT data of the conglomerate core shows high density siderite nodules within the relatively uniform (density) quartz-chert section of the core. This feature would not otherwise be apparent without physically altering the core.

A crude image extraction of a high density clast (most likely siderite) was displayed in a three dimensional perspective view.

FUTURE WORK

Image analysis of CT data that provides average properties (bulk density and effective atomic number), clast shapes, pore shapes, porosity, and fracture patterns could possibly be used to help characterize desired lithofacies.

Algorithms that identify regions of common characteristic - such as lithology - could be developed using image segmentation via a histogram technique for threshold selection or using a region-dependent technique such as erosion-dilation. Also, code for three dimensional analysis of selected features such as pore space, clasts or fracture patterns could be developed to enable extraction, rotation and views at any angle.

An investigation of the calibration of CT scanners and the problem of beam hardening is another important direction to pursue.

ACKNOWLEDGEMENTS

REFERENCES

Evans, R.D., 1955, The atomic nucleus: R.E. Krieger Publishing Company.

Herman, G.T., 1980, Image reconstruction from projections: Academic Press.

Hunt, P.K., Engler, P., and Bajsarowicz, C., 1988, Computed tomography as a core analysis tool: applications, instrument evaluation, and image improvement techniques: Journal of Petroleum Technology, 40, 1203-1210.

Krause, F.F., Collins, H.N., Nelson, D.A., Machemer, S.D., and French, P.R., 1987, Multiscale anatomy of a reservoir: geological characterization of Pembina-Cardium pool, west-central Alberta, Canada: The American Association of Petroleum Geologists Bulletin, 71, 1247.

Morgan, C.L., 1983, Basic principles of computed tomography: University Park Press.

Wang, S.Y., Aryal, S., and Gryte, C.C., 1984, Computed-assisted tomography for the observation of oil displacement in porous media: Society of Petroleum Engineers Journal, 36, 53-55.

Wellington, S.L. and Vinegar, H.J., 1987, X-ray computerized tomography: Journal of Petroleum Technology, 39, 885-898.

APPENDIX A

Processing Control Files

.low energy load file - loadl.pcf

    .job

    .input

        reel 1

        eofeot 1

        sampfm -2

        skiplen 50

        samprate 5

        line 1 20 1

        trace 30 165 1

        time 0 780

        stored 9 32 13 32

    .diskout

        filestem lener01

        sampfm 0

        subset

        time 150 780

        overflow

    .eoj

.high energy load file - loadh.pcf

    .job

    .input

        reel 1

        nskip 4003

        eofeot 2

        sampfm -2

        skiplen 50

        samprate 5

        line 1 20 1

        stored 9 32 13 32

    .diskout

        filestem hener01

        sampfm 0

        subset time 150 780

        overflow

    .eoj

.time slice file - timslcl.pcf
        .job
        .timslc
                infile lener01
                outfile lener01
                line 1 20 1
                trace 30 165
                time 150 780
                overflow
        .eoj

.high energy time slice - timslch.pcf
        .job
        .timslc
                infile hener01
                outfile hener01
                line 1 20
                trace 30 165
                time 150 780
                overflow
        .eoj